*Articles*

# The Structure of Lipoprotein(a) and Ligand-Induced Conformational Changes†

John W. Weisel,*,‡ Chandrasekaran Nagaswami,‡ John L. Woodhead,‡ Abd Al-Roof Higazi,§ William J. Cain,|| Santica M. Marcovina,⊥ Marlys L. Koschinsky,# Douglas B. Cines,○ and Khalil Bdeir○

*Department of Cell and Developmental Biology and Department of Pathology and Laboratory Medicine, University of Pennsylvania School of Medicine, Philadelphia, Pennsylvania 19104, Department of Clinical Biochemistry, Hebrew University-Hadassah Medical Centers, Jerusalem, Israel IL-91120, Department of Biological Sciences, University of Delaware, Newark, Delaware 19716, Department of Medicine, Northwest Lipid Research Laboratories, 2121 North 35th Street, Seattle, Washington 98103, and Department of Biochemistry, Queen's University, Kingston, Ontario, Canada K7L 3N6*

*Received March 19, 2001; Revised Manuscript Received July 5, 2001*

ABSTRACT: Lipoprotein(a) is composed of low-density lipoprotein linked both covalently and noncovalently to apolipoprotein(a). The structure of lipoprotein(a) and the interactions between low-density lipoprotein and apolipoprotein(a) were investigated by electron microscopy and correlated with analytical ultracentrifugation. Electron microscopy of rotary-shadowed and unidirectionally shadowed lipoprotein(a) prepared without glycerol revealed that it is a nearly spherical particle with no large projections. After extraction of both lipoprotein(a) and low-density lipoprotein with glycerol prior to rotary shadowing, the protein components were observed to consist of a ring of density made up of nodules of different sizes, with apolipoprotein(a) and apolipoprotein B-100 closely associated with each other. However, when lipoprotein(a) was treated with a lysine analogue, 6-aminohexanoic acid, much of the apolipoprotein(a) separated from the apolipoprotein B-100. In 6-aminohexanoic acid-treated preparations without glycerol extraction, lipoprotein(a) particles had an irregular mass of density around the core. In contrast, lipoprotein(a) particles treated with 6-aminohexanoic acid in the presence of glycerol had a long tail, in which individual kringles could be distinguished, extending from the ring of apolipoprotein B-100. The length of the tail was dependent on the particular isoform of apolipoprotein(a). Dissociation of the noncovalent interactions between apolipoprotein(a) and low-density lipoprotein as a result of shear forces or changes in the microenvironment may contribute to selective retention of lipoprotein(a) in the vasculature.

Lipoprotein(a) [Lp(a)][1] is a plasma lipoprotein that has been implicated as a risk factor for the development of atherosclerotic vascular disease (*1*−*3*). Lp(a) is similar in structure to low-density lipoprotein (LDL), in that it is composed of a core of apolar lipid enclosed in a predominantly phospholipid monolayer with associated glycoproteins. LDL contains a single about 500 kDa glycoprotein, apolipoprotein B-100 (apoB-100), while Lp(a) also contains apolipoprotein(a) [apo(a)] linked to apoB-100 covalently via a disulfide bond as well as through noncovalent interactions (*4*). Apo(a) is polymorphic in molecular mass, containing from 12 to 51 kringle IV-like units as well as a kringle V-like unit and an inactive protease domain homologous to those in plasminogen. Some of the kringle IV units appear to contain either strong or weak lysine binding sites that contribute to the structure of the Lp(a) particle (*5*) and to its (sub)cellular distribution (*6*−*8*) and metabolism (*9*).

Some studies indicate that Lp(a) is retained more avidly in the vasculature than is LDL (*10*), but the structural features that might contribute to this behavior have not been described. Biophysical studies of Lp(a) have revealed aspects of its structure. Lp(a) particles examined by electron microscopy appeared to be roughly circular, with no apparent differences from images of LDL (*11*). Cryoelectron microscope studies showed Lp(a) particles to be roughly spherical with a low-density core surrounded by a higher density shell, and some particle averages showed a toroidal structure (*12*). However, it was not possible to relate these observations to other properties of Lp(a). The effects of lysine analogues, different ions, and salt concentration have been determined by analytical ultracentrifugation (*13*−*15*), but there have been no corresponding electron microscope studies.

Although there have been many structural studies of LDL, there are still some puzzles concerning important aspects of

† This research was supported by Grants HL30954, HL58107, and HL60169 from the National Institutes of Health.

* To whom correspondence should be addressed. Tel: 215-898-3573. Fax: 215-898-9871. E-mail: weisel@mail.cellbio.med.upenn.edu.

‡ Department of Cell and Developmental Biology, University of Pennsylvania School of Medicine.

§ Department of Clinical Biochemistry, Hebrew University-Hadassah Medical Centers.

|| Department of Biological Sciences, University of Delaware.

⊥ Department of Medicine, Northwest Lipid Research Laboratories.

# Department of Biochemistry, Queen's University.

○ Department of Pathology and Laboratory Medicine, University of Pennsylvania School of Medicine.

[1] Abbreviations: 6-AHA, 6-aminohexanoic acid; apo(a), apolipoprotein(a); r-apo(a), recombinant apolipoprotein(a); apoB-100, apolipoprotein B-100; LDL, low-density lipoprotein; Lp(a), lipoprotein(a).

10.1021/bi010556e CCC: $20.00 
Published on Web 08/07/2001

its structure and the applicability of this information to the structure of Lp(a). The diameter of LDL particles has been reported to be anywhere between 18 and 30 nm by different investigators (*16*−*23*). Although LDL is usually assumed to be spherical, one recent cryoelectron microscopy study reported that it is disklike in shape (*19*). Another group carrying out cryoelectron microscopy and single particle analysis found that LDL particles are heterogeneous and determined the structure of the largest class of them, particles with dimensions 25 × 21 × 17.5 nm (*23*).

Relatively little is known about the disposition of apo(a) on the lipoprotein surface. There is one disulfide bond linking apo(a) to apoB-100 and a second interaction via at least one of apo(a)'s kringles. Hydrodynamic modeling of analytical ultracentrifugation experiments in which recombinant apo(a) was added to LDL suggested that the bulk of the apo(a) extends into solution with little contact with the core particle (*24*, *25*). On the other hand, X-ray scattering results were interpreted to indicate that apo(a) is located on the surface with no major domains projecting into the solution (*26*). In addition, scanning probe microscopy of Lp(a) appeared to show apo(a) as a belt extending around the core particle (*27*). Analysis of hydrodynamic measurements of Lp(a) also suggest a relatively compact structure (*13*).

Lysine analogues bind to some kringles of Lp(a). Just as lysine analogues cause conformational changes in plasminogen, Lp(a) also appears to undergo a dramatic change in the presence of 6-aminohexanoic acid (6-AHA), as demonstrated by a large decrease in its sedimentation velocity in analytical ultracentrifugation experiments (*13*). The conformational change is reversible and involves apo(a), since 6-AHA has no effect on LDL. Although these changes in the behavior of Lp(a) been extensively characterized by biophysical methods, including analysis of the effects of several lysine analogues and different solvent conditions (*14*, *15*), the specific components involved in this large-scale conformational alteration have not been characterized directly by electron microscopy, which is often useful to interpret analytical ultracentrifugation results. Oxidative modification of LDL and Lp(a) also cause diverse biochemical (*28*, *29*) and functional changes that promote atherogenesis (*30*). These oxidative modifications have received extensive biochemical study but have not received detailed scrutiny using structural approaches.

In this paper, we present electron microscope images of metal-shadowed Lp(a) and LDL particles using a modified technique that preserves their structure. We also examined the effects of changes in salt concentration and oxidation on the structure of Lp(a). The apo(a) and apoB-100 proteins were visualized following glycerol treatment of the Lp(a), which appears to partially remove lipid components. The dramatic conformational changes that occur in the presence of lysine analogues were characterized by electron microscopy, giving a physical picture to aid in interpretation of analytical ultracentrifugation results. Lp(a) particles containing different isoforms of apo(a) were visualized; under certain conditions, individual kringle units could be identified. The number of kringle units counted from the electron microscope images of each isoform was correlated with the apo(a) isoform size and kringle IV repeats determined by high-resolution sodium dodecyl sulfate (SDS)−agarose gel electrophoresis followed by immunoblotting.

## EXPERIMENTAL PROCEDURES

*Lipoproteins.* Lipoproteins were isolated from human plasma by ultracentrifugation at $d = 1.21$ g/mL. Lp(a) was isolated using lysine−Sepharose chromatography. The fraction that binds to lysine−Sepharose was brought to 7.5% CsCl (w/w) and centrifuged at 50 000 rpm for 27 h to separate Lp(a) from triglyceride-rich material. LDL was purified from the fraction that did not bind to the lysine−Sepharose as described (*31*). All lipoprotein preparations were filtered under sterile conditions, aliquoted into plastic tubes, and stored under $N_2$ at 4 °C without exposure to light in 0.01% $Na_2EDTA$, 0.1% $NaN_3$ and 1 mM benzamidine until use. The purity of Lp(a) and the apparent $M_r$ of the apo(a) were determined by SDS−PAGE (3−9% acrylamide gradient gel) stained with Coomassie Blue under reducing and nonreducing conditions (*11*). Most studies were performed using Lp(a) containing apo(a) with apparent $M_r$ ∼500 000 on SDS−PAGE (designated subject S or "control", Figure 7A) ($M_r$ 212 000 based on amino acid sequences "without carbohydrate or lipids", lane c, Figure 7B). Select studies were performed with larger and smaller Lp(a) isoforms (subjects J and D, respectively) containing apo(a) with apparent $M_r$ ∼700 000 and ∼350 000 on the basis of their migration on SDS−PAGE (Figure 7A). In each case, only one species of apo(a) was apparent on SDS−PAGE under reduced conditions. In some experiments, Lp(a) was oxidized in vitro using $CuSO_4$ as described (*32*). Briefly, EDTA was removed by dialysis, 10 μM $CuSO_4$ was added for 16 h at 22 °C, and the oxidation reaction was stopped by readdition of EDTA (final concentration 0.24 mM). The oxidation state of the Lp(a) was documented by measuring thiobarbituric acid reactive substances (*33*), and the migration of oxidized and nonoxidized Lp(a) was analyzed on 0.5% native agarose gels and detected by lipid staining (Paragon Lipoprotein "Lipo" electrophoresis kit, Beckman instruments, Inc., Fullerton, CA). All preparations studied were free of oxidized Lp(a), except those purposely oxidized. Recombinant apo(a) [r-apo(a)], 17K ($M_r$ ∼249 000) was expressed in 293 (human embryonic kidney) cells and prepared as described (*34*).

*Electron Microscopy.* Rotary-shadowed samples were prepared by spraying a dilute solution of protein (final concentration of about 25 μg/mL) in a volatile buffer (0.05 M ammonium formate at pH 7.4) and 70% glycerol onto freshly cleaved mica and rotary shadowing with tungsten or platinum followed by deposition of a carbon film in a vacuum evaporator (Denton Vacuum Co., Cherry Hill, NJ) (*35*−*37*). Unidirectional shadowing was carried out in the same way, but the stage was stationary. Tungsten was used instead of platinum for most experiments because it has a slightly smaller grain size and hence provides better resolution (*37*). All experiments were repeated several times, and many micrographs were taken of randomly selected areas to ensure that the results were reproducible and representative. All of the specimens were examined in a Philips 400 electron microscope (FEI Co., Hillsboro, OR), usually operating at 80 kV. All dimensions given have been corrected for the thin layer of metal coating the specimens.

An alternative method of preparing samples for rotary shadowing was also carried out by using a modification of the mica sandwich technique described by Mabuchi (*38*).

This approach avoids both the exposure of the sample to glycerol before fixation, thus avoiding extraction of lipid and other nonprotein components from lipoproteins, and the mechanical forces associated with spraying. A 200 $\mu$L drop of the sample was placed on a piece of Parafilm next to three separated drops of sample buffer, three drops of 2% uranyl acetate, and three drops of a rinse buffer containing 100 mM ammonium acetate in 30% glycerol. A piece of 10 $\times$ 20 mm mica was freshly cleaved into two pieces, and one piece was floated on the sample drop for about 60 s. The mica was briefly floated in turn on each of the three drops of sample buffer, two of the drops of uranyl acetate, and 40 s on the third drop. This was followed by brief contact with the three drops of rinse buffer. Then, the mica was placed face down on the second piece of mica containing 30 $\mu$L of rinse buffer on the cleaved surface. The resultant mica sandwich was briefly squeezed between two layers of filter paper to remove excess fluid. The mica containing the adsorbed sample was then placed in a vacuum evaporator and shadowed as described above.

*Determination of Apo(a) Isoform Size.* The apo(a) isoforms were determined by high-resolution SDS−agarose gel electrophoresis followed by immunoblotting, as previously reported (*39*). We have evaluated the relationship between the number of apo(a) kringle IV units, as determined by pulsed-field gel electrophoresis (*40*), and the mobility of the isoforms on SDS−agarose gel electrophoresis and found that the logarithm of the kringle IV number was highly correlated with the mobility of the isoforms on agarose gels (*41*). The relative mobility of the bands was used to determine the number of kringle IV units in the sample, and it was calculated in comparison to a standard with known apo(a) sizes. The standard was prepared in-house by combining the plasma of three individuals chosen on the basis that they covered a large range of apo(a) isoforms, 13, 19, 24, 32, 38 kringle IV units, as assessed by pulsed-field gel electrophoresis (*40*). A UMAX Powerlook III scanner (UMAX Technologies, Inc.) was used to transform photographic films into image files that were then analyzed with gel analysis software (Sigma Gel, SPSS Application Package). The apo(a) isoforms in the samples were therefore designated by the relative number of kringle IV units.

*Analytical Ultracentrifugation.* Sedimentation velocity experiments were performed on a Beckman Optima XL-I ultracentrifuge using an An-60 Ti four-place rotor containing double-sector cells equipped with 12 mm aluminum-filled Epon centerpieces and sapphire windows. A rotor speed of 30 000 rpm was used with the temperature controlled at 25 °C. Sedimentation data were obtained using the Rayleigh interference optical system, and weight average sedimentation coefficients were computed using the time derivative method (*42*). The sedimentation boundaries were analyzed using version 5.01 of the Svedberg software program developed by Philo (*43*). This involved the application of a modified Fujita−MacCosham curve fitting function to the boundary data to produce multiple-species fits.

## RESULTS

*Electron Microscopy of Shadowed Lipoprotein(a). (A) The Shape of Lp(a) and LDL.* Several different methods were used to prepare shadowed Lp(a) for examination by electron microscopy. Typically, preparations of proteins for shadowing are vacuum-dried in the presence of glycerol to reduce surface tension and avoid drying artifacts. However, glycerol is commonly used to solubilize membrane components for the purpose of making cell membranes permeable (*44*). Therefore, since glycerol will extract lipid and other nonprotein components from lipoproteins, we also carried out experiments using a sandwich technique (*38*), modified to eliminate glycerol exposure to the samples until after fixation, as described in Experimental Procedures. Fixation was accomplished by using uranyl acetate, which is a particularly good fixative for lipoproteins (*45*).

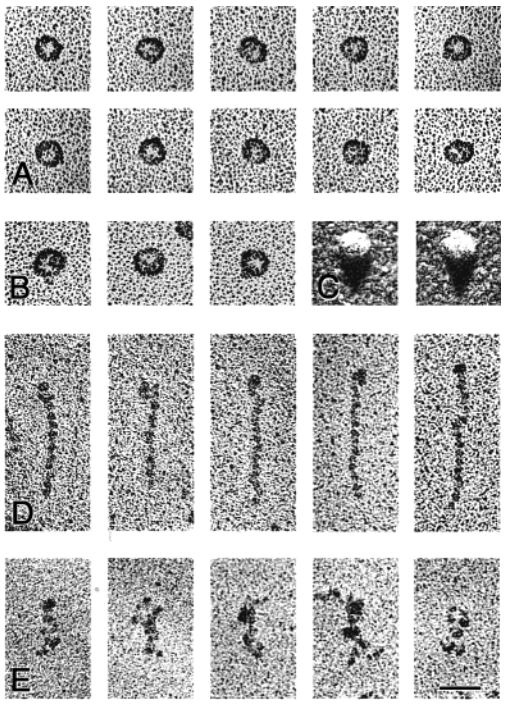


FIGURE 1: Electron microscopy of rotary-shadowed Lp(a) at different ionic strengths prepared in the absence of glycerol, unidirectionally shadowed Lp(a), and rotary-shadowed recombinant apo(a). (A) Rotary-shadowed Lp(a) in 100 mM ammonium acetate buffer prepared on a surface with uranyl acetate fixation before exposure to glycerol. (B) Rotary-shadowed Lp(a) prepared in the same way as in (A) but in 10 mM ammonium acetate buffer. (C) Unidirectionally shadowed Lp(a) prepared on a surface with uranyl acetate fixation before exposure to glycerol. Note that the contrast in this image has been reversed so that it is opposite that in all other images to make the shadows dark. (D) Rotary-shadowed r-apo(a) sprayed in the presence of glycerol. Examples of elongated strands consisting of small nodules with a larger nodule at one end. (E) Rotary-shadowed r-apo(a) sprayed in the presence of glycerol. Examples of more compact structures. Samples in images A and B were shadowed with platinum, while those in images C−E were shadowed with tungsten. Bar = 50 nm.

Lp(a) prepared using this sandwich technique (glycerol added post fixation) usually appeared in projection as a roughly circular or oval structure with greatest density at the edges gradually decreasing toward the center (Figure 1A). In some images, the density in the center of the ring was greater than in others, so that these structures appeared to be filled rather than open circles. These structures had dimensions of 25.4 $\pm$ 1.8 nm by 22.1 $\pm$ 1.7 nm. As indicated by these measurements, the particles were generally somewhat oval shaped rather than circular; the ratio of long to short dimensions was 1.15 $\pm$ 0.05. However, there were no projections from the surface of the particles, even though

the technique of rotary shadowing is particularly suitable for visualizing any portion of the polypeptide chain that could be extending from the Lp(a) core. Therefore, the apo(a) must be closely associated with the surface of the LDL particle.

Because ionic strength has an effect on the sedimentation rate of Lp(a), we also examined Lp(a) under lower salt conditions (10 mM ammonium acetate) to visualize this change (Figure 1B). Under these conditions, the Lp(a) particles appeared to have somewhat rougher, more irregular, and more dense edges, and their average diameters were 28.2 ± 2.4 nm by 24.3 ± 2.3 nm, about 11% larger than the same particles at higher salt concentration.

*(B) Is Lp(a) a Sphere or a Disk?* Previous structural studies of Lp(a) and LDL revealed roughly circular structures, but since electron microscope images are typically projections of structures, there has been a continued controversy as to whether these lipoproteins are truly spherical or disk shaped (*12*, *16*, *19*−*23*). On a practical basis, the difference between these two possibilities is that spherical structures would have the same height as their diameter, while the height of disklike structures would be substantially less than their diameter. Therefore, we used unidirectional shadowing to determine the height of Lp(a) and LDL (Figure 1C). Measurement of many particles revealed that the ratio of height to shortest dimension of both Lp(a) and LDL was about 0.85. In conclusion, Lp(a) is roughly spherical.

*(C) Visualization of the Protein Components of Lp(a) and LDL and Isolated Apo(a).* Commonly used methods of preparing biological samples for electron microscopy involve diluting the macromolecules or particles into a volatile buffer that contains a large percentage of glycerol. Lp(a) and LDL that were prepared in this way and then sprayed onto freshly cleaved mica and rotary shadowed with tungsten were examined by electron microscopy. We found that glycerol treatment of lipoproteins removed nonprotein components so that the protein alone was visible in electron micrographs.

LDL particles prepared by this method had the general appearance of a circular ring with a mean diameter of 27.6 ± 3.2 nm and an outer diameter of 35.1 ± 2.8 nm (Figure 2B). The rings were each composed of several different-sized nodules. The number and arrangement of nodules around each ring were somewhat variable, but there were commonly a large nodule, one or two medium nodules, and several smaller ones. The diameter of this ring was greater than the known diameter of LDL particles, indicating that the apoB-100 had retained its circular shape but had expanded following the extraction of nonprotein components.

Glycerol treatment of Lp(a) also removed nonprotein components so that the protein was visible (Figure 2A). Examination of Lp(a) preparations revealed a circular ring with a mean diameter of 29.7 ± 3.3 nm and an outer diameter of 37.2 ± 3.2 nm, made up of several different-sized nodules. The number and arrangement of nodules around each ring were again somewhat variable, but there were commonly about three large nodules and numerous smaller ones. The ring was the same size as that of LDL, although its thickness and density were greater, indicating that the apo(a) of Lp(a) was closely associated with apoB-100. In some images, strands were separated over part of the ring to give the appearance of a double ring, but in most cases there was a single ring that was considerably more dense than that seen in LDL. The presence of apo(a) in the ring was confirmed by monoclonal antibodies to apo(a), which bound to the rings of Lp(a) but not to LDL rings (data not shown).

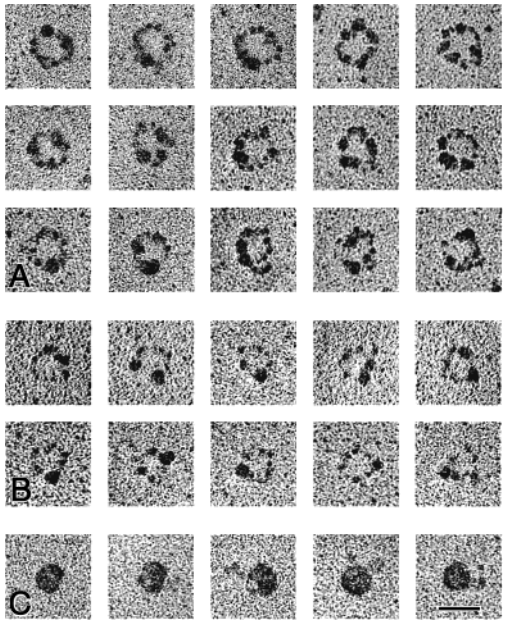


FIGURE 2: Electron microscopy of rotary-shadowed Lp(a), LDL, and oxidized Lp(a) in the presence of glycerol. (A) Lp(a) rotary-shadowed with tungsten prepared by spraying in 0.05 mM ammonium formate buffer with glycerol. (B) Rotary-shadowed LDL prepared in the same way. (C) Lp(a) oxidized by treatment with $CuSO_4$ and rotary shadowed for electron microscopy in the same way. Bar = 50 nm.

For comparison, apo(a) by itself was also examined using this approach. Recombinant apo(a) containing 17 kringle IV repeats, in addition to the protease domain and kringle V, was sprayed onto freshly cleaved mica in the presence of glycerol and examined by electron microscopy (Figure 1D,E). Some molecules appeared as linear chains of small nodules with a larger nodule at one end (Figure 1D). The average length of the chains was 89 ± 16 nm. Counting the number of nodules together with the measured lengths of the extended apo(a) chains indicated that the nodules each had an average spacing of 7.7 ± 0.5 nm and that there were an average of 11.6 nodules/apo(a), including the single larger nodule at one end. These results suggest that there was variable or partial unfolding of the apo(a), presumably attributable to noncovalent kringle−kringle interactions, since this apo(a) has a total of 19 units, 17 kringle IV repeats, one kringle V, and a protease domain.

In other cases, the chains appeared to be more compact or tangled to form somewhat irregular globular structures (Figure 1E). Most of these more compact structures appeared to be folded versions of the completely linear structures but were about half as long or less.

*(D) The Shape of Oxidized Lp(a).* Studies were performed to examine the effect of oxidation on the structure of Lp(a). For this purpose, Lp(a) was oxidized in vitro using $CuSO_4$ for 16 h at 22 °C and prepared for electron microscopy by a variety of methods. In all cases, the oxidized Lp(a) particles appeared to be circular disks with a diameter of 27.2 ± 1.4 × 24.9 ± 2.0 nm (Figure 2C). Thus, these particles were about the same size as Lp(a) in the absence of glycerol. In contrast to normal Lp(a), where lipid was extracted to reveal the protein (Figure 2A), the particles were more similar to

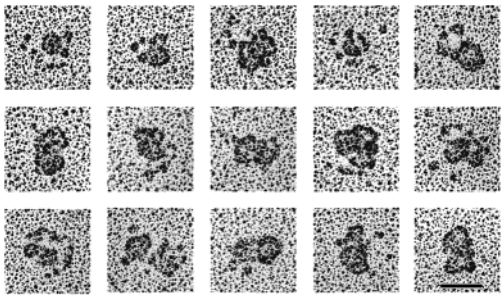

FIGURE 3: Effect of 6-AHA on the conformation of Lp(a). Lp(a) rotary shadowed with platinum in the presence of 6-AHA prepared on a surface with uranyl acetate fixation before exposure to glycerol. Bar = 50 nm.

Lp(a) fixed prior to exposure to glycerol. That is, there was little difference in the appearance of oxidized Lp(a) whether they had been treated with glycerol. The process of oxidation appears to stabilize the lipid−protein structure so that there was little change in the presence of glycerol. However, there were some rough edges consisting of small projections from the core and some less dense regions in the core or apparent holes where material had been extracted.

*Ligand-Induced Conformational Changes of Lipoprotein-(a) and Different Isoforms of Apo(a).* The lysine analogue, 6-aminohexanoic acid (6-AHA), was added to Lp(a) to determine its effect on the interactions between apo(a) and the remainder of the Lp(a) complex. Lp(a) particles treated with 100 mM 6-AHA and prepared on a surface in the absence of glycerol were examined by electron microscopy (Figure 3). These images show a striking change in structure, reflecting a large-scale conformational change induced by this lysine analogue. Instead of the relatively uniform circular structures described previously, these particles were irregular in shape. In some cases, there was a large increase in diameter and an increase in apparent surface roughness. In others, a variety of types of projections emanated from the central dense region.

Lp(a) particles that were treated with 100 mM 6-AHA in solution and then prepared in the typical way for rotary shadowing, by spraying a dilute solution of protein in the presence of a high concentration of glycerol, were again different in appearance (Figures 4 and 5A). Most Lp(a) particles treated with 100 mM 6-AHA and glycerol in solution and sprayed appeared as a circular ring with a long tail extending from the ring. About 85% of the particles under these conditions had tails, while the remainder did not. The circular portion of these structures was commonly composed of a large nodule, one or two medium nodules, and several smaller ones and had an average diameter of 28.4 ± 2.8 nm and an outer diameter of 35.8 ± 2.8 nm. The tails were made up of small nodules and had an average length of 91 ± 20 nm. The nodules were spaced 7.7 ± 0.2 nm apart and on average each chain contained 11.8 ± 2.5 nodules.

In many preparations, the tails were oriented in a single direction over a small area of electron microscope grid (Figure 4). The reason for the presence of locally oriented tails was apparent in cases in which the edge of a dried glycerol drop was visible, where the tails were seen to be oriented perpendicular to the drop edge, or in a radial direction with respect to the drop.

Note that the Lp(a) in Figure 4 was shadowed with platinum, whereas the particles visualized in Figure 5 were shadowed with tungsten. The contrast is higher with platinum, so that the nodules in the tails were visualized more clearly (Figure 4). On the other hand, the resolution of molecules shadowed with tungsten is slightly higher, so that the smaller nodules in the apoB-100 ring were better visualized (Figure 5).

Lp(a) particles were also treated in a similar way with other concentrations of 6-AHA. Lp(a) treated with 10 or 100 mM 6-AHA appeared superficially to be similar. In fact, measurements of the lengths of the tails in 10 mM 6-AHA revealed that the average lengths were 88 ± 20 nm, nearly identical to those seen in the presence of 100 mM 6-AHA (Figure 6D). However, only about 55% of the particles had visible tails. On the other hand, 97% of the particles had tails in preparations carried out in the presence of 200 mM 6-AHA.

Lp(a) particles with different isoforms of apo(a) were sprayed onto mica in the presence of glycerol and 6-AHA and visualized by electron microscopy. Lp(a) with two isoforms of apo(a) different from the control shown in Figure

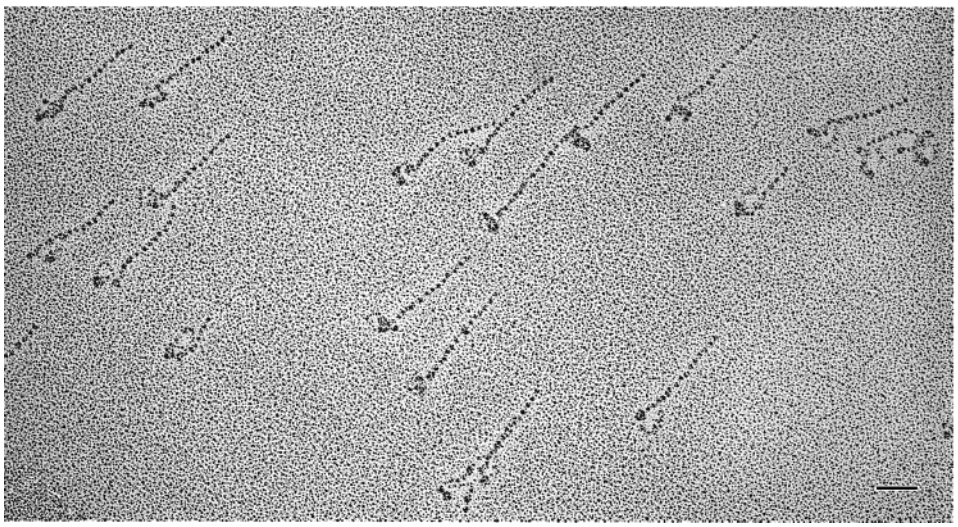

FIGURE 4: Electron microscopy of rotary-shadowed Lp(a) in the presence of 6-AHA and glycerol. A field of Lp(a) particles prepared by spraying in 0.10 M ammonium acetate and 0.20 M 6-AHA in the presence of glycerol and rotary shadowing with platinum. These experiments show the extension and orientation of the apo(a) tails. Bar = 50 nm.

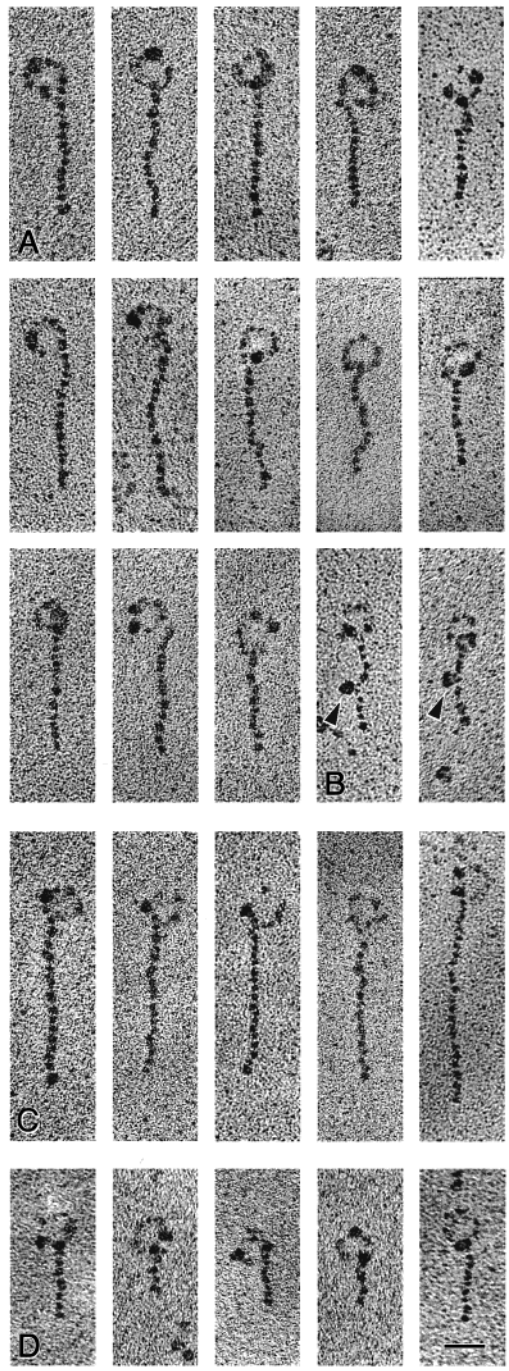


FIGURE 5: Effect of 6-AHA on the conformation of Lp(a) and visualization of Lp(a) with different apo(a) isoforms. All of these samples were sprayed in 0.05 M ammonium formate, 0.10 M 6-AHA, and glycerol and rotary shadowed with tungsten. (A) Lp(a) (from the control subject S). (B) Lp(a) with antibodies to apo(a), indicated by arrowheads. (C) Lp(a) with a different isoform of apo(a) (from subject J). (D) Lp(a) with another isoform of apo(a) (from subject D). Bar = 50 nm.

5A have tails with strikingly different lengths (Figure 5C,D). The tail lengths were measured for the different isoforms, and histograms of the resulting measurements are shown in Figure 6. The apo(a) tails of the control Lp(a) (subject S) had a mean length of 91 ± 20 nm (or about 11.8 ± 2.5 nodules per chain), with 89% of the tails in the range of 60−120 nm length (6.5−15.6 nodules) (Figure 6A). The mean length of apo(a) tails from subject J was 150 ± 32 nm (or about 19.5 ± 4.1 nodules per chain), with a less homogeneous distribution of the tail length (70−210 nm) in comparison to subject S (Figure 6B), and that of subject D was 55 ± 14 nm (an average of 7.1 ± 1.8 nodules per chain), with 92% of the tails in the range of 30−80 nm length (3.9−10.3 nodules) (Figure 6C). For comparison, the histogram of the measured lengths of recombinant apo(a), with 17 kringle IV units, is also shown (mean length = 81 ± 16 nm) (Figure 6E).

The apo(a) component of Lp(a) from subject S comigrated with LDL ($M_r$ ~500 000) under reducing conditions (Figure 7A), whereas apo(a) from subject J migrated at apparent $M_r$ ~700 000 and that from subject D migrated at ~300 000−400 000. Thus, the number of nodules/chain correlated closely with the molecular masses of the different isoforms of apo(a), as determined on reduced SDS−PAGE. To confirm the correlation between the size of apo(a) (kringle number) and the number of nodules visualized by electron microscopy, plasma from subjects S and J was phenotyped for apo(a) size isoform. The apo(a) isoforms were determined by a high-resolution SDS−agarose gel electrophoresis followed by immunoblotting. The relative mobility of the bands was used to determine the number of kringle IV units in each sample and was calculated in comparison with a standard with known apo(a) sizes as described in Experimental Procedures. The results show that apo(a) from subject S contains 14 kringle IV repeats and that from subject J contains 17 kringle IV repeats. The molecular masses of apo(a) from subjects S and J, calculated on the basis of the number of the kringle IV repeats and the known amino acid sequences (not including carbohydrate or lipids), were 212 000 and 249 000, respectively.

*Ligand-Induced Conformational Changes Studied by Analytical Ultracentrifugation.* The conformational changes in Lp(a) induced by lysine analogues were also examined by analytical ultracentrifugation. Although this approach has been used previously (*13*, *14*), it was necessary to repeat such analyses under the buffer conditions that we required for electron microscopy. Representative sedimentation velocity boundaries plotted as interference fringe displacement versus apparent sedimentation coefficient ($s^*$) are shown in Figure 8. In the absence of 6-AHA, time derivative analysis of the sedimentation data (*42*) gave a weight-average sedimentation coefficient of 12.5 S after correction to standard conditions ($s_{20,w}$). The average sedimentation coefficient decreased to 11.2 S in the presence of 10 mM 6-AHA and to 9.9 S in 100 mM 6-AHA.

The analytical ultracentrifugation results were also analyzed by applying a modified Fujita−MacCosham multiple-species fit to the data (*43*). The best multiple-species fit to the Lp(a) data in the absence of 6-AHA (circles in Figure 8) indicated that 88% of the particles were present in a single monomeric form with an $s_{20,w}$ value of 12.2 S. There also appeared to be a small amount of aggregation under these conditions with 9% dimers (17.6 S) and 3% trimers (24.1 S). This concurs with our electron microscope observations that indicated that the majority of the particles in the absence of 6-AHA were monomeric and fairly uniform in appearance (Figure 1A), whereas there was a small degree of aggregation of Lp(a) particles (not shown). For Lp(a) in 10 mM 6-AHA (diamonds in Figure 8), the multiple-species fitting procedure produced a best fit for about a 50:50 mixture of a 12.3 S and a 10.3 S monomeric species with no evidence for significant aggregation. The Lp(a) sedimentation data in 100

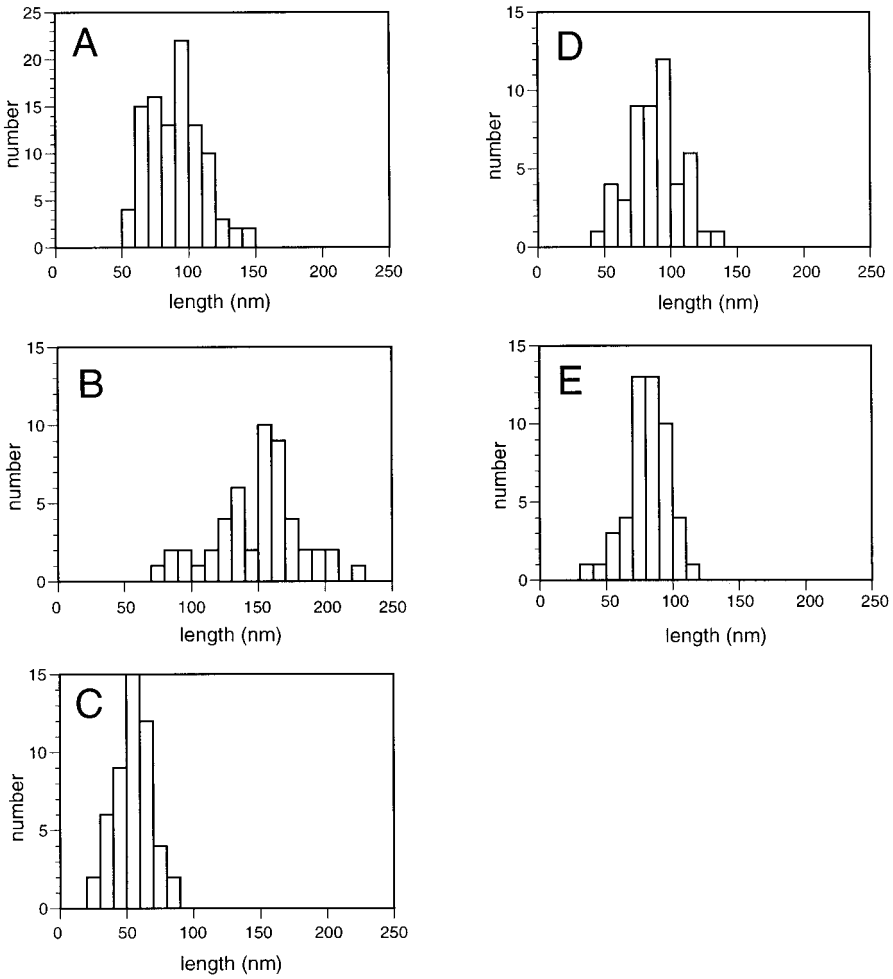


FIGURE 6: Histograms of the lengths of tails of Lp(a) in the presence of 6-AHA. These histograms show the distributions of lengths of apo(a). (A) Lengths of the tails of the control Lp(a) used for most of these experiments (subject S) in the presence of 100 mM 6-AHA. The molecular mass of apo(a) from SDS−agarose gel electrophoresis was 212 000. (B) Lengths of the tails in the presence of 100 mM 6-AHA of Lp(a) from subject J containing apo(a) with molecular mass of 249 000. (C) Lengths of the tails in the presence of 100 mM 6-AHA of Lp(a) from subject D containing apo(a) with molecular mass of 150 000. (D) Lengths of the tails of the control Lp(a) in the presence of 10 mM 6-AHA. (E) Lengths of recombinant apo(a) chains with molecular mass of 249 000.

mM 6-AHA (squares in Figure 8) produced a best fit for a 20:80 mixture of a 12.3 and a 9.5 S monomeric species. Sedimentation velocity provides a measure of the average conformation of each particle. Since a single particle can be in a state of internal equilibrium with one or more of its conformational isomers, the equilibrium constant gives a measure of the proportion of time it spends in each major conformation. If a particle is considered to spend most of its time in one or the other of two conformational states (and not much time in the intermediate forms), then the system can be approximated by a two-species system consisting of a mixture of the two end-point monomers. Comparison with the electron microscope results described above indicates that there is very good agreement with these modeling results, where the system appears to consist of a mixture of a relatively compact form of Lp(a) and an extended form (with a resultant lower sedimentation coefficient). The decrease from 10.3 to 9.5 S for the extended species is consistent with a slightly more open conformation in 100 mM 6-AHA than in 10 mM 6-AHA.

## DISCUSSION

*The Structure of Lp(a).* We first considered the structure of LDL, which we assumed would be more homogeneous and less complex than that of Lp(a). Previous studies of LDL by electron microscopy utilizing the technique of negative contrast or, more recently, cryomicroscopy, revealed a roughly circular structure with a diameter of about 18−30 nm (*16*, *19*−*21*, *23*, *46*). It is not possible to distinguish protein from lipid or other components with the method of negative contrast, although monoclonal antibodies have been used to localize certain specific segments of the apoB-100 protein on the surface of LDL (*17*, *18*). On the other hand, analysis of LDL by cryoelectron microscopy, which does enable protein to be distinguished from lipid, revealed that apoB-100 is indeed located on the surface of the particle and appears to form two rings around the lipid core (*19*, *20*).

Examination of unstained, frozen, hydrated Lp(a) by cryoelectron microscopy revealed several somewhat different sizes and shapes of particles (*12*). Analysis of the density profile of the circular structures indicated that there was a layer of protein on the surface, and a toroidal structure was observed in averages of one class of particles. In another study, a recombinant apo(a) was examined by analytical ultracentrifugation and electron microscopy and characterized; interactions between r-apo(a) and LDL were also detected (*25*).

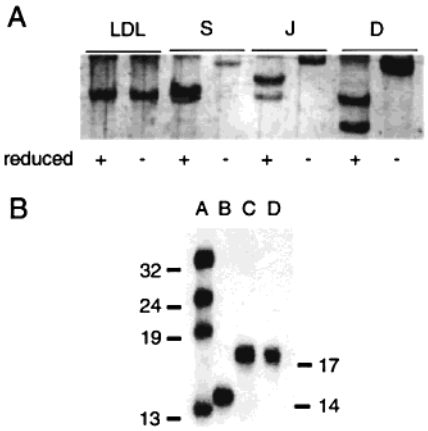


FIGURE 7: Gel electrophoresis of Lp(a) with different isoforms of apo(a). (A) Coomassie Blue stained slab gel of LDL control and Lp(a)s from three individuals with different Lp(a) isoforms (subjects S, J, and D) which were analyzed using SDS−PAGE with a 3−9% gradient of acrylamide under reduced and nonreduced conditions. The gel with LDL on the left shows the position of apoB-100; the same band is present in each of the Lp(a) under reduced conditions. (B) Apo(a) isoform size as determined by SDS−agarose gel electrophoresis followed by immunoblotting as described in Experimental Procedures. The apo(a) isoforms are designated by the relative number of kringle IV units. (A) Standard with apo(a) isoforms determined by pulsed-field gel electrophoresis; (B) sample S (14 kringle IV units); (C) sample J (17 kringle IV units); (D) recombinant apo(a) (17 kringle IV units).

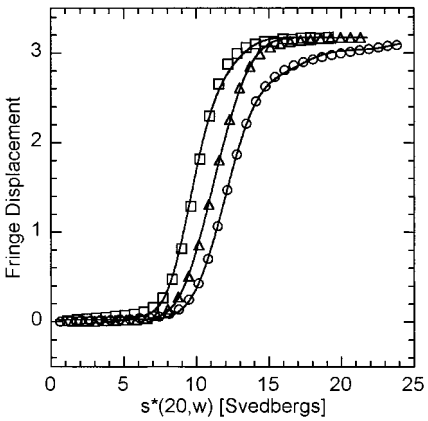


FIGURE 8: Effect of 6-AHA on the sedimentation of Lp(a). Data from representative sedimentation velocity boundaries in 100 mM ammonium acetate buffer are denoted by circles (absence of 6-AHA), triangles (10 mM 6-AHA), and squares (100 mM 6-AHA). Multiple-species fits to each boundary using the modified Fujita−MacCosham function are indicated by solid lines.

Examination of the same particle systems by electron microscopy using different preparation techniques has proven useful because the strengths and weaknesses of different approaches are often complementary. We employed the technique of rotary shadowing with a thin coating of metal but also used a variant method of preparation to avoid extraction of lipid by the glycerol that is normally present to prevent drying artifacts. Lp(a) was prepared using a sandwich technique, which allowed the particles to be fixed prior to addition of glycerol, which is still necessary during drying to prevent artifacts.

Lp(a) prepared in this way revealed circular structures very similar to those seen by negative contrast or cryoelectron microscopy. In most cases, the particles consisted of roughly circular rings with greater density at the outer edge. This is just the sort of image that would be expected from shadowing of a sphere. Metal would accumulate under the edge of the lower hemisphere sitting on the mica surface, as well as on the upper hemisphere. Because of the shape of a sphere, more metal will accumulate around the outer edge (equator) than toward the middle (poles). Therefore, more electrons will be scattered around the outer edge, giving rise to images of circular rings. With more accumulation of metal, the upper pole will be covered more thoroughly, giving rise to the filled circles.

At lower salt concentration, the particles had somewhat rougher, more irregular, and denser edges and a slightly larger average diameter. These results are consistent with those from analytical ultracentrifugation experiments, which gave a maximum *s* value for Lp(a) of 12.5 S at 100−200 mM salt and a value of 10.5 S in the absence of salt (*13*). The higher *s* value indicates a more compact form, whereas the lower value is consistent with the somewhat larger diameter and a more irregular surface seen in our micrographs.

In addition, we found that use of the standard rotary-shadowing preparation of spray drying in the presence of glycerol without fixation prior to shadowing revealed new structural information about Lp(a). Glycerol extracts nonprotein components from Lp(a) in solution, enabling the protein to be examined in relative isolation. However, other methods of extracting nonprotein components from LDL, for example, revealed an elongated apoB-100 structure that had lost its circular appearance (*16*, *46*). In contrast, the circular appearance was retained if the samples were fixed prior to extraction. Apparently, the nonprotein components help to maintain the association between apoB-100 and apo(a), but the basic shape of the apoB-100 is maintained when the other components are extracted under mild conditions. The rings of apoB-100 are made up of nodules of various sizes. However, every apoB-100 molecule contains a single large nodule, which probably corresponds to the globular amino-terminal domain. The locations of specific sequences of apoB-100 on the surface of LDL have been mapped by immunoelectron microscopy, showing that apoB-100 forms a ribbon or belt around the circumference of the LDL (*17*, *18*), consistent with our results.

Although the apoB-100 of the LDL and Lp(a) retained its circular shape following glycerol treatment, these circles have a larger diameter than the LDL and Lp(a) particles themselves. However, the mapping of apoB-100 on LDL revealed a kink in the ribbon (*18*). Thus, it could be that, with glycerol extraction of lipid, the apoB-100 becomes unkinked. Although uncoiling of this kink probably cannot account for the entire difference in circumference, it is likely that the remainder may be the result of additional, smaller bends or kinks or a result of perturbation of the hydrophobic interactions involving the surface proteins that normally maintain its structure.

In the presence of glycerol, images of Lp(a) are similar to those of LDL, with a ring of protein of the same diameter but with greater density and containing more large nodules. These results demonstrate that apo(a) is closely associated with the surface of Lp(a) and closely associated with apoB-100. Previous studies using recombinant apo(a) added back to LDL appeared to show the apo(a) extending out from the surface of the LDL, but these images may have arisen as a result of incomplete binding of apo(a) to LDL. In contrast,

our results are entirely consistent with results from analytical ultracentrifugation (*13*), X-ray scattering (*26*), and scanning probe microscopy (*27*) experiments and results that define the parts of apo(a) and apoB-100 that interact with each other (*47*).

The cellular and molecular mechanisms underlying the atherogenic action of LDL and Lp(a) involve in part the occurrence of an oxidative modification of both the lipid and the protein components of the lipoproteins (*10*, *28*, *48*, *49*). Oxidation of LDL and Lp(a) affects the catabolism of the lipoproteins, including changes in receptor recognition, catabolic rate, retention in the vessel wall, and propensity to accelerate atherosclerosis (*10*, *50*−*53*). Electron microscopy of oxidized Lp(a) demonstrated that lipid was not extracted by glycerol, leading to the conclusion that lipid may be cross-linked to the protein or trapped by the protein cross-linking or more tightly bound because of chemical changes during oxidation. These structural changes may accompany the loss of recognition of oxidized LDL and Lp(a) by LDL receptors and the acquisition of particle recognition and uptake by scavenger receptors leading to foam cell formation and lipid retention in the vessel wall (*10*, *53*, *54*).

*Characterization of Conformational Changes of Lp(a) Induced by Lysine Analogues.* Lp(a) undergoes a dramatic conformational change on treatment with lysine analogues, such as 6-AHA. These changes have been characterized by the method of analytical ultracentrifugation (*13*−*15*). This conformational change, characterized by up to almost a 50% decrease in sedimentation coefficient, is one of the largest of any ligand-induced conformational change measured to date. However, although analytical ultracentrifugation is an accurate method to characterize changes in large, complex structures such as Lp(a), more than one interpretation can be placed on these results. There are many different shapes (for a given mass) that produce similar sedimentation coefficients. Conversely, a relatively small conformational change in a critical location can produce a large change in the sedimentation properties. It is therefore very important that interpretation of sedimentation properties be carried out in conjunction with direct morphological examination (e.g., by electron microscopy) to avoid misleading conclusions. The electron microscope images presented here provide a physical picture of the changes in the particle recorded by the analytical ultracentrifugation approach.

The nature of the conformational change has been demonstrated by electron microscopy of the Lp(a) in the presence of 6-AHA. Apo(a) normally lies in the outer shell of the Lp(a) particle and is attached to apoB-100 via a disulfide bond between $Cys^{4326}$ of apoB-100 and $Cys^{4057}$ in kringle IV9 of apo(a) (*55*, *56*) and interacts noncovalently with apoB-100 via one or more lysine binding sites of the apo(a) kringles (*47*, *57*). Lp(a) particles treated with 6-AHA without glycerol extraction show a very complex and irregular array of nodules around their circumference. Thus, this conformational change does not involve complete extension of the apo(a) but neither is there a simple increase in the diameter of the sphere.

Since it was necessary to study the conformation of Lp(a) by electron microscopy using buffer conditions that differed from those used by others for analytical ultracentrifugation, we repeated this analysis. Lp(a) sedimented at 12.5 S under our buffer conditions. In 10 mM 6-AHA the $s_{20,w}$ value decreased to 11.2 S and further decreased to 9.9 S in 100 mM 6-AHA. The conformational change is thus titratable and proportional to the concentration of 6-AHA. Since these results are very similar to those analytical ultracentrifugation results reported previously (*13*), our electron microscope results can be used to interpret both sets of sedimentation results. Both electron microscope and analytical ultracentrifugation results can be modeled as a mixture of two species, with similar ratios of compact and extended forms. The appearance of Lp(a) by electron microscopy suggests that the conformational change in any one particle is all or none, with a mixture of two different forms at low concentrations of 6-AHA. As the concentration of 6-AHA is increased, all particles undergo the conformational change. The sedimentation coefficient provides a single value related to the average amount of time spent in the various conformations. To determine the conformational equilibrium constant by observing a single particle, this particle would have to be visualized over a period of time to observe the proportion of time spent in each state. The electron microscope images give a moment frozen in time, reflecting the probability of an individual particle being in a particular conformation at any given time. However, this is directly related to the sedimentation results, since the proportion of time any one particle would spend in a given conformation, as measured by sedimentation, is directly related to the overall fraction of particles with that conformation within the whole population at any time, as measured by electron microscopy.

Lp(a) particles treated with 6-AHA in the presence of glycerol differ dramatically in appearance. Most of the apo(a) moieties are much more obvious because they extend directly out from the remainder of the circular core particle, which is the apoB-100 chain. In many cases, the apo(a) chains were aligned in a certain direction in a limited region of the electron microscope grid. In cases where the edge of a dried glycerol drop was visible, the tails were oriented perpendicular to the edge or in a radial direction with respect to the drop. This observation suggests that forces present during the drying of the droplets, such as the surface tension of the retreating liquid−vapor front, extend and align the tails. It is also possible that the lipid components of Lp(a) contribute to the interaction of apo(a) with the LDL surface, and the extended conformation of apo(a) in the presence of 6-AHA was observed in Lp(a) prepared with glycerol because of the extraction of lipid from the LDL.

There is a clear difference in the density of the circular core from Lp(a) examined in the presence of 6-AHA, which is readily accounted for by the fact that the apo(a) is no longer interacting with the apoB-100. Thus, apo(a) normally interacts strongly with apoB-100, so that in the presence of glycerol, where extraction of lipid occurs, a single ring is seen. Only in the presence of lysine analogues do the two chains separate, as a consequence of disruption of the noncovalent interactions between kringles and apoB-100. The biological settings in which the noncovalent interactions between apo(a) and apoB-100 may dissociate are unknown, as are the implications for apo(a) retention or activity in the vasculature. It is possible that binding of Lp(a) to cell surfaces, fibrin, or the extracellular matrix via lysine binding sites (*8*, *58*) induces comparable alterations in the conformation of the apo(a) with respect to LDL. Exposure of the

kringles may affect plasminogen activation, binding to fibrin, and binding to cell surface receptors or cause other alterations in biologically important processes. On the other hand, such a conformational change may expose the LDL particle of the Lp(a) and make it more available for recognition by known LDL receptors such as LRP or LDL-r.

Initially, analytical ultracentrifugation studies suggested that there were two apo(a) chains per Lp(a) (*59*). However, careful analysis of amino acid data clearly indicated that there is only one apo(a) molecule per particle (*60*). Subsequent ultracentrifugation studies, taking into account the binding of solvent components to Lp(a), then led to the same conclusion (*61*). The electron micrographs of glycerol-treated rotary-shadowed Lp(a) presented here demonstrate unequivocally that there is a single apo(a) attached to each Lp(a).

The concentration of 6-AHA necessary to observe the conformational change by electron microscopy was considerably less than that necessary to cause similar changes in the previous analytical ultracentrifugation experiments (*13*). This difference has been accounted for by the effects of different anions on the conformation of Lp(a) (*14*). Whereas most of the previous analytical ultracentrifugation experiments were performed in the presence of $Cl^-$ ions, our electron microscope experiments were carried out in a volatile buffer without $Cl^-$. Since $Cl^-$ ions likely stabilize the association of the apo(a) with the Lp(a) backbone, in their presence a higher concentration of 6-AHA is necessary for the conformational change (*14*).

In the images of the apo(a) tails, there was often substructure visible. Most commonly, the tails consisted of strings of small nodules at regular intervals. Each of these nodules appears to correspond to a single kringle. They are similar in appearance to the nodules seen in plasminogen by electron microscopy (*62*). The same nodules are seen on the extended recombinant apo(a) chains (Figure 1D). These images are similar to electron micrographs of negatively contrasted apo(a) (*24*). However, the kringles are more clearly and consistently visualized in our micrographs using shadowed metal for contrast. In contrast to calculations from the negatively contrasted images (*24*), the kringle spacing that we determined, about 7.7 nm/kringle, is larger. However, each repeat includes not only a kringle but also connecting polypeptide chains, as well as increased size arising from the coating of shadowed metal. Compact forms of apo(a) visualized in these experiments (Figure 1E) may display intermolecular interactions similar to those of apo(a) in 6-AHA-treated Lp(a), which has a complex array of apo(a) surrounding the core.

Individual kringles and/or domains can be counted in the apo(a) chains of the 6-AHA-treated Lp(a), permitting the part of polypeptide chain still associated with the apoB-100 to be estimated. We observed a close correlation between the lengths of the tails (i.e., the number of nodules) observed by electron microscopy for recombinant apo(a) and each of three natural Lp(a) isoforms we examined and their migration on SDS−PAGE. High-resolution SDS−agarose gel electrophoresis followed by immunoblotting was used to determine apo(a) isoform size and kringle IV repeats for Lp(a) from the subjects tested and to confirm the correlation.

Although examination of the recombinant apo(a) shows significant heterogeneity in the length of the tails, the fully extended form was not observed. This finding suggests that there are multiple potential interactions within apo(a), some of which are not susceptible to 6-AHA. The most fully extended conformation contains 14 nodules although the molecules contain 19 individual units (protease domain, kringle V, and 17 kringle IV repeats). The heterogeneity in the length of the tails of naturally occurring Lp(a) was considerably greater and correlated directly with the size of the isoform (subject J > S > D). This finding may imply that LDL alters the strength of the interkringle interactions in apo(a) or that more than one of the kringle IV repeats in the larger isoforms may interact with apoB and thereby are obscured from view. Similar conclusions of more than one class of noncovalent association between apo(a) kringle IV types 6−8 and the LDL surface have been described by testing the binding of a battery of r-apo(a)s to human LDL (*57*). It is necessary to be cautious in evaluating these calculations because the measured lengths of the apo(a) molecules are likely to be underestimates, since some of the "extended" chains may still be partially folded. Such partial unfolding likely accounts for the greater heterogeneity in the length of the tails visualized by electron microscopy than can be accounted for by variation in isoforms on SDS−PAGE.

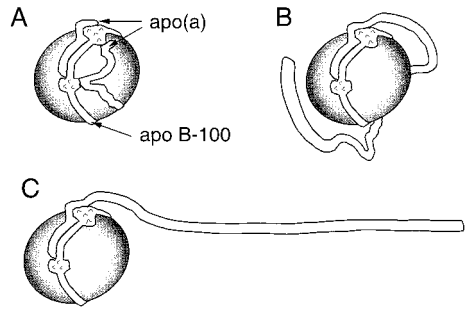


FIGURE 9: Schematic diagram of Lp(a) and ligand-induced conformational changes. (A) Lp(a) in the absence of lysine analogues. The apo(a) is closely associated with the apoB-100 on the surface of the roughly spherical particle. (B) Lp(a) in the presence of lysine analogues. The apo(a) remains covalently attached to apoB-100 but moves away from the particle surface. (C) Lp(a) in the presence of lysine analogues and other mechanical forces that yield a fully extended linear chain.

The conformational change in Lp(a) in the presence of lysine analogues can be interpreted by analysis of all of these results together. Under normal circumstances, the apo(a) is very closely associated with the apoB-100 on the surface of the Lp(a), bound by a disulfide bond and one or more kringle interactions with the embedded apoB-100 (shown schematically in Figure 9A). In the presence of carboxyl-terminal lysines or lysine analogues, the strength of the interactions between apo(a) and apoB-100 is weakened, allowing apo(a) to move away from the surface of the Lp(a) (Figure 9B). The apo(a) remains fairly close to the surface but still contributes to a large increase in hydrodynamic radius, as a result of increased surface roughness, resulting in a higher frictional drag in analytical ultracentrifugation experiments. Although the apo(a) remains relatively close to the surface under most conditions, including analytical ultracentrifugation where the rate of particle movement is quite slow, apo(a) can become fully extended by mechanical forces (Figure 9C). For example, the shearing forces present in arterial blood flow may cause extension of the apo(a). The extended apo(a) tails could then present the kringle binding sites and/or

the LDL particle to matrix components, cellular receptors, and associated atherosclerotic plaque in a more exposed form. Recent studies suggest that the lysine binding heterogeneity of plasma Lp(a) is not primarily an intrinsic property of the Lp(a) but rather results from the ability of apo(a) to noncovalently associate with abundant plasma components such as LDL and fibronectin (*63*). Such association of Lp(a) with proteins in blood flow might be a physiological setting in which the large-scale conformational changes in the Lp(a) particle could take place.

We conclude from these studies that the structure of Lp(a) is exquisitely sensitive to environmental conditions. Changes in salt concentration cause visible changes in the diameter of the particles and surface appearance, but the differences are still relatively small. There is a large conformational change in the presence of lysine analogues, one of the largest protein conformational changes so far discovered and characterized. With the added forces of drying in these experiments and possibly in flowing blood, there is a further and dramatic large-scale change to a fully extended chain. The distribution and the extent of these conformational changes correlate with the size of the apo(a) isoform and 6-AHA concentration. Analogous changes in the behavior of apo(a) in vivo may contribute to the variation in the strength of the association between the apo(a) size and the risk of cardiovascular disease. Identification of the factors that may modify apo(a) conformation in vivo may provide a new approach to modifying the impact of this risk factor. Similar conformational changes in von Willebrand factor (*64*) induced by shear stress or in vitronectin upon interaction with other macromolecules (reviewed in ref *65*), for example, are associated with increased cell/matrix binding and alterations in their biologic activity. Additional studies are required to examine the pathophysiological consequences of the observed changes in Lp(a) structure.

## ACKNOWLEDGMENT

We thank Gabriela Canziani for technical assistance with analytical ultracentrifugation experiments and Walter F. Stafford for help in interpretation of these results.

## REFERENCES

1. Bostom, A. G., Cupples, L. A., Jenner, J. L., Ordovas, J. M., Seman, L. J., Wilson, P. W. F., Schaefer, E. J., and Castelli, W. P. (1996) *J. Am. Med. Assoc. 276*, 544−548.
2. Assmann, G., Schulte, H., and von Eckardstein, A. (1996) *Am. J. Cardiol. 77*, 1179−1184.
3. Danesh, J., Collins, R., and Peto, R. (2000) *Circulation 102*, 1082−1085.
4. Koschinsky, M. L., and Gabel, B. R. (1998) *Biochemistry 37*, 7892−7898.
5. Ernst, A., Helmhold, M., Brunner, C., Pehtro-Schramm, A., Armstrong, V. W., and Muller, H.-J. (1995) *J. Biol. Chem. 270*, 6227−6234.
6. Miles, L. A., Sebald, M. T., Fless, G. M., Scanu, A. M., Curtiss, L. K., Plow, E. F., and Hoover-Plow, J. L. (1998) *Fibrinolysis Proteolysis 12*, 79−87.
7. Keesler, G. A., Gabel, B. R., Devlin, C. M., Koschinsky, M. L., and Tabas, I. (1996) *J. Biol. Chem. 271*, 32096−32104.
8. Boonmark, N. W., Lou, X.-J., Yang, Z. J., Schwartz, K., Zhang, J.-L., Rubin, E. M., and Lawn, R. M. (1997) *J. Clin. Invest. 100*, 558−564.
9. Argraves, K. M., Kozarsky, K. F., Fallon, J. T., Harpel, P. C., and Strickland, D. K. (1997) *J. Clin. Invest. 100*, 2170−2181.
10. Nielsen, L. B. (1999) *Atherosclerosis 143*, 229−243.
11. Edelstein, C., Italia, J. A., Klezovitch, O., and Scanu, A. M. (1996) *J. Lipid Res. 37*, 1786−1801.
12. Sines, J., Rothnagel, R., van Heel, M., Gaubatz, J. W., Morrisett, J. D., and Chiu, W. (1994) *Chem. Phys. Lipids 67/68*, 81−89.
13. Fless, G. M., Furbee, J., Snyder, M. L., and Meredith, S. C. (1996) *Biochemistry 35*, 2289−2298.
14. Fless, G. M., Furbee, J., Snyder, M. L., and Meredith, S. C. (1997) *Biochemistry 36*, 11304−11313.
15. Fless, G. M., Halfman, C. J., and Kirk, E. W. (2000) *Biochemistry 39*, 2740−2747.
16. Phillips, M. L., and Schumaker, V. N. (1989) *J. Lipid Res. 30*, 415−422.
17. Chatterton, J. E., Phillips, M. L., Curtiss, L. K., Milne, R. W., Marcel, Y. L., and Schumaker, V. N. (1991) *J. Biol. Chem 266*, 5955−5962.
18. Chatterton, J. E., Phillips, M. L., Curtiss, L. K., Milne, R., Fruchart, J.-C., and Schumaker, V. N. (1995) *J. Lipid Res. 36*, 2027−2037.
19. Antwerpen, R. V., and Gilkey, J. C. (1994) *J. Lipid Res. 35*, 2223−2231.
20. Antwerpen, R. V., Chen, G. C., Pullinger, C. R., Kane, J. P., LaBelle, M., Krauss, R. M., Luna-Chavez, C., Forte, T. M., and Gilkey, J. C. (1997) *J. Lipid Res. 38*, 659−669.
21. Spin, J. M., and Atkinson, D. (1995) *Biophys. J. 68*, 2115−2123.
22. Spring, D. J., Chen-Liu, L. W., Chatterton, J. E., Elovson, J., and Schumaker, V. N. (1992) *J. Biol. Chem. 267*, 14839−14845.
23. Orlova, E. V., Sherman, M. B., Chiu, W., Mowri, H., Smith, L. C., and Gotto, A. M. (1999) *Proc. Natl. Acad. Sci. U.S.A. 96*, 8420−8425.
24. Phillips, M. L., Lembertas, A. V., Schumaker, V. N., Lawn, R. W., Shire, S. J., and Zioncheck, T. F. (1993) *Biochemistry 32*, 3722−3728.
25. Phillips, M. L., Lembertas, A. V., Schumaker, V. N., Lawn, R. W., Shire, S. J., and Zioncheck, T. F. (1994) *Chem. Phys. Lipids 67/68*, 91−97.
26. Prassl, R., Schuster, B., Abuja, P. M., Zechner, M., Kostner, G. M., and Laggner, P. (1995) *Biochemistry 34*, 3795−3801.
27. Xu, S. (1998) *Biochemistry 37*, 9284−9294.
28. Prassl, R., Schuster, B., Laggner, P., Flamant, C., Nigon, F., and Chapman, M. J. (1998) *Biochemistry 37*, 938−944.
29. Beaudeu, J.-L., Cesarini, M.-L., Gardes-Albert, M., Maclouf, J., Merbal, R., Esposito, B., Peynet, J., and Tedgui, A. (1997) *Atherosclerosis 132*, 29−35.
30. Steinberg, D. (1999) *J. Clin. Invest. 103*, 1487−1488.
31. Rader, D. J., Cain, W., Ikewaki, K., Talley, G., Zech, L. A., Usher, D., and Brewer, H. B. (1994) *J. Clin. Invest. 93*, 2758−2763.
32. Liu, S. Y., Choy, S., Dembinski, T. C., Hatch, G. M., Mymin, D., Shen, G. X., Angel, A., Choy, P. C., and Man, R. Y. K. (1994) *Cardiovasc. Res. 28*, 1476−1481.
33. Harats, D., Dabach, D., Hollander, G., Ben-Naim, M., Schwartz, R., Berry, E. M., Stein, O., and Stein, Y. (1991) *Atherosclerosis 90*, 127−139.
34. Koschinsky, M. L., Tomlinson, J. E., Zioncheck, T. F., Schwartz, K., Eaton, D. L., and Lawn, R. M. (1991) *Biochemistry 30*, 5044−5051.
35. Fowler, W. E., and Erickson, H. P. (1979) *J. Mol. Biol. 134*, 241−249.
36. Weisel, J. W., Stauffacher, C. V., Bullitt, E., and Cohen, C. (1985) *Science 230*, 1388−1391.
37. Veklich, Y. I., Gorkun, O. V., Medved, L. V., Nieuwenhuizen, W., and Weisel, J. W. (1993) *J. Biol. Chem. 268*, 13577−13585.
38. Mabuchi, K. (1991) *J. Struct. Biol. 107*, 22−28.
39. Marcovina, S. M., Zhang, Z. H., Gaur, V. P., and Albers, J. J. (1993) *Biochem. Biophys. Res. Commun. 191*, 1192−1196.
40. Lackner, C., Boerwinkle, E., Leffert, C. C., and Hobbs, H. H. (1991) *J. Clin. Invest. 87*, 2153−2161.
41. Marcovina, S. M., Hobbs, H. H., and Albers, J. J. (1996) *Clin. Chem. 42*, 436−439.

42. Stafford, W. F. (1994) in *Methods in Enzymology. Numerical Methods. Part B*, pp 478−501, Academic Press, Orlando, FL.
43. Philo, J. S. (1996) *Biophys. J. 72*, 435−444.
44. Squire, J. (1981) *The Structural Basis of Muscular Contraction*, p 89, Plenum Press, New York.
45. Hayat, M. A. (2000) *Principles and Techniques of Electron Microscopy*, pp 345−347, Cambridge University Press, Cambridge.
46. Zampighi, G., Reynolds, J. A., and Watt, R. M. (1980) *J. Cell Biol. 87*, 555−561.
47. Gabel, B. R., McLeod, R. S., Yao, Z., and Koschinsky, M. L. (1998) *Arterioscler., Thromb., Vasc. Biol. 18*, 1738−1744.
48. Naruszewicze, M., Giroux, L. M., and Davignon, J. (1994) *Chem. Phys. Lipids 67/68*, 167−174.
49. Palinski, W., Rosenfeld, M. E., Yla-Herttuala, S., Gurtner, G. C., Socher, S. S., Butler, S. W., Parthasarathy, S., Carew, T. E., Steinberg, D., and Witztum, J. L. (1989) *Proc. Natl. Acad. Sci. U.S.A. 86*, 1372−1376.
50. Sambrano, G. R., Parthasarathy, S., and Steinberg, D. (1994) *Proc Natl. Acad. Sci. U.S.A. 91*, 3265−3269.
51. Pekelharing, H. L., Kleinveld, H. A., Duif, P. F., Bouma, B. N., and van Rijn, H. J. (1996) *Blood Coagulation Fibrinolysis 7*, 641−649.
52. Kramer-Guth, A., Greiber, S., Pavenstadt, H., Quaschning, T., Winkler, K., Schollmeyer, P., and Wanner, C. (1996) *Kidney Int. 49*, 1250−1261.
53. Quinn, M. T., Parthasarathy, S., Fong, L. G., and Steinberg, D. (1987) *Proc. Natl. Acad. Sci. U.S.A. 84*, 2995−2998.
54. Parthasarathy, S., Quinn, M. T., Schwenke, D. C., Carew, T. E., and Steinberg, D. (1989) *Arteriosclerosis 9*, 398−404.
55. Callow, M. J., and Rubin, E. M. (1995) *J. Biol. Chem. 270*, 23914−23917.
56. Brunner, C., Kraft, H.-G., Utermann, G., and Muller, H.-J. (1993) *Proc. Natl. Acad. Sci. U.S.A. 90*, 11643−11647.
57. Gabel, B. R., and Koschinsky, M. L. (1998) *Biochemistry 37*, 7892−7898.
58. Liu, J.-N., Kung, W., Harpel, P. C., and Gurewich, V. (1998) *Biochemistry 37*, 3949−3954.
59. Fless, G. M., Snyder, M. L., Furbee, J., Garcia-Hedo, M.-T., and Mora, R. (1994) *Biochemistry 33*, 13492−13501.
60. Albers, J. J., Kennedy, H., and Marcovina, S. M. (1996) *J. Lipid Res. 37*, 192−196.
61. Fless, G. M., and Santiago, J. Y. (1997) *Biochemistry 36*, 233−238.
62. Weisel, J. W., Nagaswami, C., Korsholm, B., Petersen, L. C., and Suenson, E. (1994) *J. Mol. Biol. 235*, 1117−1135.
63. Xia, J., May, L. F., and M. L., K. (2000) *J. Lipid Res. 41*, 1578−1584.
64. Siedlecki, C. A., Lestini, B. J., Kottke-Marchant, K., Eppell, S. J., Wilson, D. L., and Marchant, R. E. (1996) *Blood 88*, 2939−2950.
65. Preissner, K. T., and Seiffert, D. (1998) *Thromb. Res. 89*, 1−21.

BI010556E